# G3(MP2) Study of the $C_3H_6O^{+\bullet}$ Isomers Fragmented from 1,4-Dioxane$^{+\bullet}$

**Chow-Shing Lam and Wai-Kee Li***

*Department of Chemistry, The Chinese University of Hong Kong, Shatin, N.T., Hong Kong*

**See-Wing Chiu***

*National Center for Supercomputing Applications, University of Illinois, Champaign, Illinois 61820*

*Received: May 4, 2005; In Final Form: June 19, 2005*

The fragmentation process of ionized 1,4-dioxane and the reactions between the $C_3H_6O^{+\bullet}$ ions, one of the major fragments, and various reactants (including acetonitrile, formaldehyde, ethylene, and propene) have been studied experimentally with mass spectrometry. In the present work, G3(MP2) calculations were carried out to investigate these processes theoretically. In agreement with experiment, isomers $CH_3OCHCH_2^{+\bullet}$ (**1**) and $^{\bullet}CH_2CH_2OCH_2^+$ (**2**) were found to be the $C_3H_6O^{+\bullet}$ ions fragmented from ionized 1,4-dioxane, with **2** being the major product. The mechanisms of the formation of **1** and **2** were successfully established. In addition, the characteristic reactivities, as well as the corresponding reaction mechanisms, of both isomers were rationalized with the aid of calculations. Finally, a minor reaction between isomer **2** and propene was identified, and the presence of the product of this reaction was found to be useful in explaining the aforementioned mass spectrometric data.

## 1. Introduction

The chemistry of $C_3H_6O^{+\bullet}$ radical cations has been extensively studied both experimentally and theoretically.[1−12] These radical cations, in numerous isomeric forms, appear in the mass spectra of many organic compounds, such as 1,4-dioxane, 4-methyl-1,3-dioxolane, etc. More importantly, the $C_3H_6O^{+\bullet}$ ionic systems participate in a wide range of rearrangement and dissociative processes.[7,8,12] In the $C_3H_6O^{+\bullet}$ family, distonic ions deserve special attention because unique properties result from its separation of charge and radical sites. For instance, the unimolecular and bimolecular reactions of the distonic ion, $^{\bullet}CH_2CH_2OCH_2^+$, have been thoroughly explored.[13−16] In many of these experiments, this radical cation was generated by the fragmentation reaction of ionized 1,4-dioxane.[13−15]

Distonic ion $^{\bullet}CH_2CH_2OCH_2^+$ had been assumed to be the sole component of the *m*/*z* 58 ions fragmented from 1,4-dioxane$^{+\bullet}$ until its fragmentation pattern was revisited by Thissen et al.[17] In their work, the results of the ion−molecule reactions between $C_3H_6O^{+\bullet}$ fragments and selected reactants, including acetonitrile, formaldehyde, propene, and labeled ethylene, show that the *m*/*z* 58 ions fragmented from 1,4-dioxane$^{+\bullet}$ are composed of both $CH_3OCHCH_2^{+\bullet}$ (**1**) and $^{\bullet}CH_2CH_2OCH_2^+$ (**2**). Contrary to previous assumptions, isomer **1** constitutes about 7% of the $C_3H_6O^{+\bullet}$ radical cations formed, playing the role of a minor component.

In this work, we used the G3(MP2) method,[18] which was successfully employed in the studies of different chemical systems by our group,[19−21] to investigate the pathways of the reactions involved in the study of Thissen et al.[17] It is hoped that our results will make clear the respective reactivity of isomers **1** and **2**. More importantly, the computational results will help to establish the mechanism for the formation of the minor component **1**.

## 2. Theoretical Methods

All calculations reported here were carried out using the Gaussian98 and Gaussian03 packages of programs.[22] The G3(MP2) level of theory was applied to obtain the energies of the molecular species studied in this work. In this theory, prior to energetic calculations, the geometry of a species is optimized at the B3LYP/6-31++G(d) level.[23−26] To determine the energy $E_e$ of a structure, two single-point calculations at the levels of QCISD(T)/6-31G(d) and MP2/G3MP2large are carried out. In addition, the empirical higher-level correction (HLC) and the zero-point vibrational energy (ZPVE) correction are also applied. The B3LYP/6-31++G(d) vibrational frequencies, scaled by 0.964, are applied for the ZPVE correction at 0 K ($E_0 = E_e +$ ZPVE). Because all of the structures were optimized at the B3LYP/6-31++G(d) level, instead of the conventional MP2(Full)/6-31G(d) level, the energetic results are better denoted as G3(MP2)//B3LYP. However, for simplicity, they are called G3(MP2) in the following discussions. For the systems studied in this work, the error bar of this method should be less than $\pm 15$ kJ mol$^{-1}$.[19−21]

All stable structures were confirmed by their harmonic vibrational calculations yielding no imaginary frequency, while each transition structure (TS) was established by its one and only imaginary frequency. For most of the TSs, the "reactants" and "products" were confirmed by intrinsic reaction coordinate (IRC) calculations.[27,28] In case of IRC failure, such as IRC calculations for certain rotational TSs, the TS was judicially modified according to the transition vector and then its reactants and products were obtained by following the downward paths from TS. Additionally, natural bond orbital (NBO)[29] analyses were carried out at the B3LYP/6-31++G(d) level to determine the bonding in certain molecular species.

10.1021/jp0523064 CCC: $30.25 
Published on Web 07/20/2005

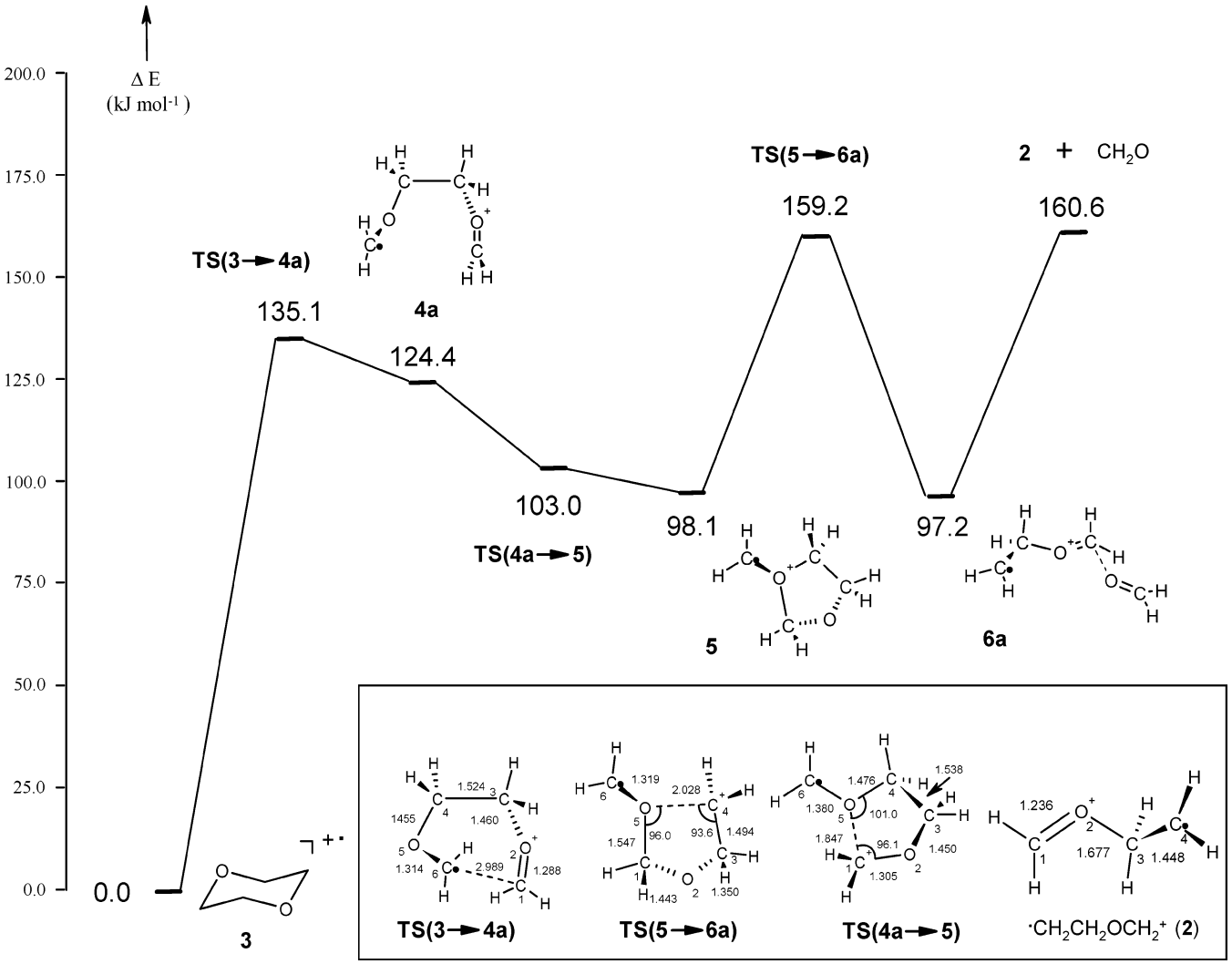


**Figure 1.** G3(MP2) potential energy surface showing the mechanism of reaction 1, $C_4H_8O_2^{+\bullet}$ (**3**) → $^{\bullet}CH_2CH_2OCH_2^+$ (**2**) + $CH_2O$.

## 3. Results and Discussion

The respective G3(MP2) potential energy surfaces (PESs) for the reactions studied are shown in Figures 1−12. In each PES, selected optimized structural parameters of some important intermediates, TSs, or both are also displayed. The optimized structures of all species involved in all of the reactions studied are available in the Supporting Information. Throughout this paper, bond lengths are given in angstroms and bond angles are in degrees. In addition, the G3(MP2) energetic data ($E_0$ and $H_{298}$) of all of the species are also included in the Supporting Information.

**3.1. Formation of $C_3H_6O^{+\bullet}$ Isomers 1 and 2 via Fragmentation of 1,4-dioxane$^{+\bullet}$ (3).** The equations of these processes are

$$C_4H_8O_2^{+\bullet}\,(\mathbf{3}) \rightarrow {}^{\bullet}CH_2CH_2OCH_2^{+}\,(\mathbf{2}) + CH_2O \qquad (1)$$

$$C_4H_8O_2^{+\bullet}\,(\mathbf{3}) \rightarrow CH_3OCHCH_2^{+\bullet}\,(\mathbf{1}) + CH_2O \qquad (2)$$

There are three possible pathways for reaction 1 and their G3(MP2) profiles are shown in Figures 1 and 2, while that of reaction 2 is displayed in Figure 3. The calculated ionization energy of 1,4-dioxane is 9.11 eV, in fairly good agreement with the experimental values of 9.19 ± 0.01 eV[9] and 9.058 eV (73 062 ± 4 $cm^{-1}$).[30] As can be seen in Figure 1, ionized 1,4-dioxane (**3**) has a calculated barrier of 135.1 kJ $mol^{-1}$ for ring opening via homolytic C−C bond cleavage transition structure, **TS(3 → 4a)**. Afterward, intermediate **4a** cyclizes again to form a five-membered ring species, **5**, via **TS(4a → 5)**. While IRC calculations confirm that **TS(4a → 5)** links species **4a** and **5**, the G3(MP2) calculations of these species show that the TS lies below ion **4a** in energy [at the level employed for geometry optimization, B3LYP/6-31++G(d), **TS(4a → 5)** lies above **4a** and **5** by 15.4 and 2.6 kJ $mol^{-1}$, respectively]. Then dioxolane-like ion **5** undergoes ring opening via **TS(5 → 6a)** to yield ion−molecule complex (IMC) **6a**. It is worthy to note that, in forming **6a** from **TS(5 → 6a)**, the $C^1-O^5$ bond is automatically cleaved after the fission of the $C^4-O^5$ bond. It can be seen that **6a** is composed of ion **2** and formaldehyde and that the interaction between them is purely electrostatic, according to NBO analysis.

Radical cation **2** is formed by the dissociation of IMC **6a** and this process requires 63.4 kJ $mol^{-1}$. Therefore, the sum of the G3(MP2) energy of **2** and formaldehyde relative to **3** (160.6 kJ $mol^{-1}$ or 1.66 eV) and the calculated ionization energy (IE) of 1,4-dioxane (9.11 eV) is taken as the calculated appearance energy (AE) of $C_3H_6O^{+\bullet}$. The computed G3(MP2) energy sum of 10.77 eV is in fair agreement with the experimental AE result of 10.56 eV.[9] It is noted that the more recent report of the IE of 1,4-dioxane by Burrill and Johnson[30] does not include the AE of $C_3H_6O^{+\bullet}$.

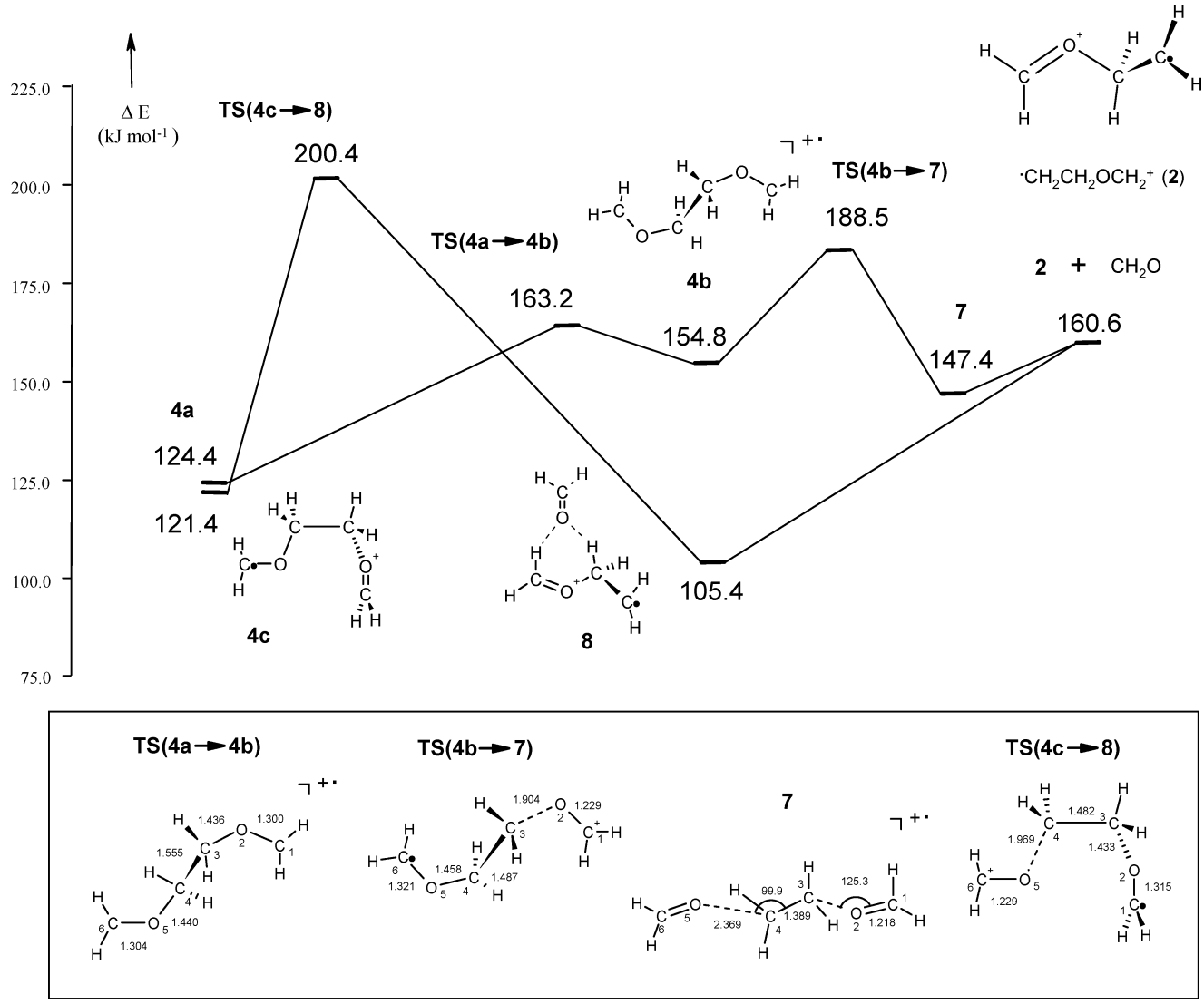


**Figure 2.** G3(MP2) potential energy surface showing the mechanism for reaction 1, $C_4H_8O_2^{+\bullet}$ (**3**) → $^{\bullet}CH_2CH_2OCH_2^+$ (**2**) + $CH_2O$.

Though the calculated result is in fair agreement with the experimental value, this pathway is complicated by reaction 5 (to be discussed later in section 3.3.1), which is an addition−cyclization process between ion **2** and formaldehyde. As will be seen in Figure 6, IMC **6b**, a conformer of **6a** can undergo this reaction with a small overall barrier. In contrast, IMC **6a** requires about 60 kJ mol$^{-1}$ to produce free ion **2**. As a result, the formation of the *m*/*z* 58 ions is unlikely to be competitive with reaction 5, which yields *m*/*z* 88 and *m*/*z* 87 ions. In other words, the pathway shown in Figure 1 is probably not the *major* source of ion **2**. Upon further investigation, two alternative pathways were established for producing ion **2**. As shown in Figure 2, ion **2** can be produced by direct C−O cleavage of the conformers of **4a**, **4b**, and **4c**, followed by the dissociation of the complexes yielded. Though the G3(MP2) barriers (200.4 and 188.5 kJ mol$^{-1}$ above **3**, respectively) are higher than the previous pathway, these pathways are suggested to be more efficient in producing ion **2**. This is because, when the parent ion, **3**, is converted to any stable intermediate, the excess energy gained from electron impact ionization may easily be lost by collision. Partial cleavage of a C−O bond in **4b** via **TS(4b → 7)** produces species **7**. This species is not considered to be an IMC because the two equivalent C−O bonds, 2.369 Å in length, are very weakly bonding according to NBO analysis. Then **7** dissociates into products **2** and $CH_2O$. On the other hand, intermediate **4c**, which has a stability comparable to that of intermediate **4a**, can undergo a C−O bond cleavage via **TS(4c → 8)**. Because complete C−O bond cleavage is required to form IMC **8**, it is expected that **TS(4c → 8)** is higher than **TS(4b → 7)** in energy. Because the overall barriers of these two pathways (shown in Figure 2) differ by less than 12 kJ mol$^{-1}$, both processes may be considered to be the major sources of **2**.

The *β*-distonic ion **2** had been assumed to be the only component of the $C_3H_6O^{+\bullet}$ (*m*/*z* 58) fragment. From the NBO analysis of the results, it can be seen that the $C^1-O^2$ bond is essentially a double bond. Also, because of the delocalization of the unpaired electron from radical center $C^4$ into $\sigma^*(C^3-O^2)$, the $C^3-O^2$ bond (1.677 Å) is considerably longer than an ordinary C−O bond, which is usually about 1.43 Å. The weakened $C^3-O^2$ bond is closely related to the reactivity of **2**. This will be further discussed later in this paper.

Thissen et al.[17] suggested that $CH_3OCHCH_2^{+\bullet}$ (**1**) was formed via a fomaldehyde-catalyzed 1,3-H transfer within an IMC in the dissociation channel of 1,4-dioxane$^{+\bullet}$. This hypothesis is based on the absence of deuterated isomer **1**, $CD_3OCDCD_2^{+\bullet}$ in $C_3D_6O^{+\bullet}$ ions fragmented from ionized 1,4-dioxane-$d_8$. Though isotopic effect is seldom so strong that it prohibits a process, this observation suggests that hydrogen transfer is a

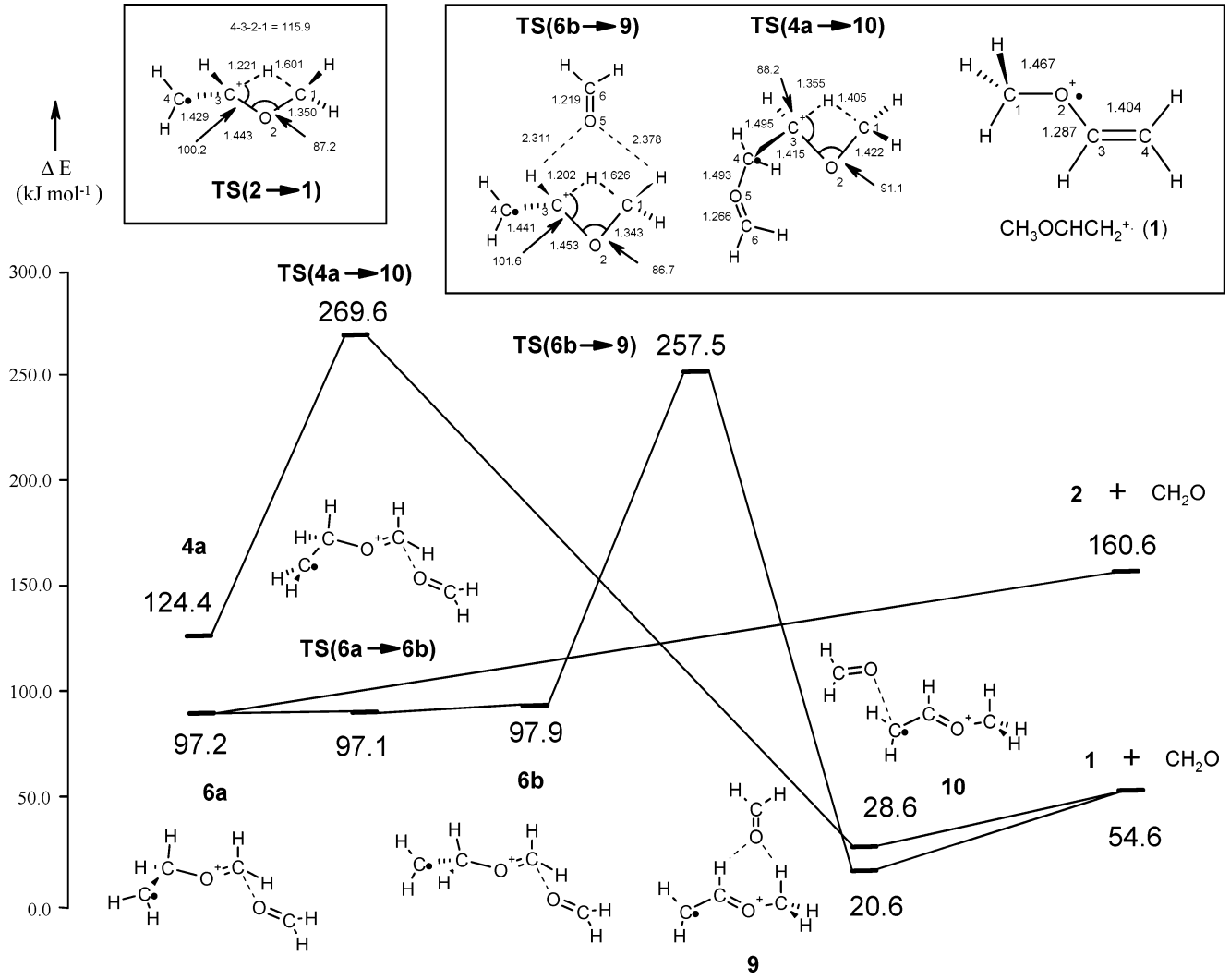


**Figure 3.** G3(MP2) potential energy surface showing the mechanism for reaction 2, $C_4H_8O_2^{+\bullet}$ (**3**) → $CH_3OCHCH_2^{+\bullet}$ (**1**) + $CH_2O$.

rate-determining step for the generation of isomer **1**. We have constructed the reaction according to this hypothesis, as shown in Figure 3. The key TS of this reaction, **TS(6b → 9)** for the 1,3-H transfer, has been successfully identified, and the possible pathway for the formation of **1** has been established. From the energy profile displayed in Figure 3, it can be seen that **TS(6b → 9)** connects IMC **6b** and **9**. The former, which is essentially another conformer of IMC **6a**, can dissociate into **2** and formaldehyde, while the dissociation of **9** yields **1** and formaldehyde. It is noted that **TS(6b → 9)** is very high in energy, being 257.5 kJ $mol^{-1}$ above the parent ion, **3**.

To verify the catalysis by formaldehyde, we also investigated the possibility of the isomerization of ion **2** to **1** and successfully located the corresponding **TS(2 → 1)** (see Figure 3), which is also a TS for the 1,3-H transfer. The energy barrier for this isomerization is 153.6 kJ $mol^{-1}$, which is similar to that of **TS(6b → 9)** (159.6 kJ $mol^{-1}$). The formation of IMC **6b** (with formaldehyde participation) does not provide a lower energy barrier for the isomerization step, the energy sum of **TS(2 → 1)** and formaldehyde is 314.2 kJ $mol^{-1}$ above the parent ion, **3**. Though the overall energy barrier is 56.8 kJ $mol^{-1}$ higher than that of the previous mechanism, this difference is actually about the same as the energy gained by complex formation of IMC **6a** (63.4 kJ $mol^{-1}$). That is to say, **TS(6b → 9)** is essentially the "complex" formed by **TS(2 → 1)** and formaldehyde. Therefore, formaldehyde does not catalyze the formation of **1** at all. In other words, our G3(MP2) calculations do not support the important role of formaldehyde in the formation of **1** first suggested by Thissen et al.[17]

Moreover, for IMC **6b**, isomerization via **TS(6b → 9)** again is not competitive with the aforementioned reaction 5. Hence, ion **1** cannot be produced if the hydrogen shift does not take place in an earlier stage of the dissociation of the parent ion, **3**. In view of this, we attempted to locate a H-shift TS prior the formation of IMC. Finally, **TS(4a → 10)** was identified. The barrier of this TS is 269.6 kJ $mol^{-1}$, which is similar to that of **TS(6b → 9)**. Upon examining **TS(4a → 10)**, one can see that the hydrogen shift is accompanied by the C−O bond cleavage. After IMC **10** is formed, it can readily dissociate into **1** and $CH_2O$. This process is facile because the formation of this complex only provides a stabilization of 26.0 kJ $mol^{-1}$. This pathway is also displayed in Figure 3.

Because of the huge energy barrier, isomer **1** constitutes a very small portion (∼5−10%) of the $C_3H_6O^{+\bullet}$ fragment ions. It is known that deuterium substitution may slow, sometimes considerably, such a process (formation of **1**).[31] Hence, it is possible that an unfavorable process of this kind is effectively shut down by deuterium substitution. The formation of **1** is solely the result of the enormous energy gained from electron impact ionization, not the catalysis of formaldehyde.

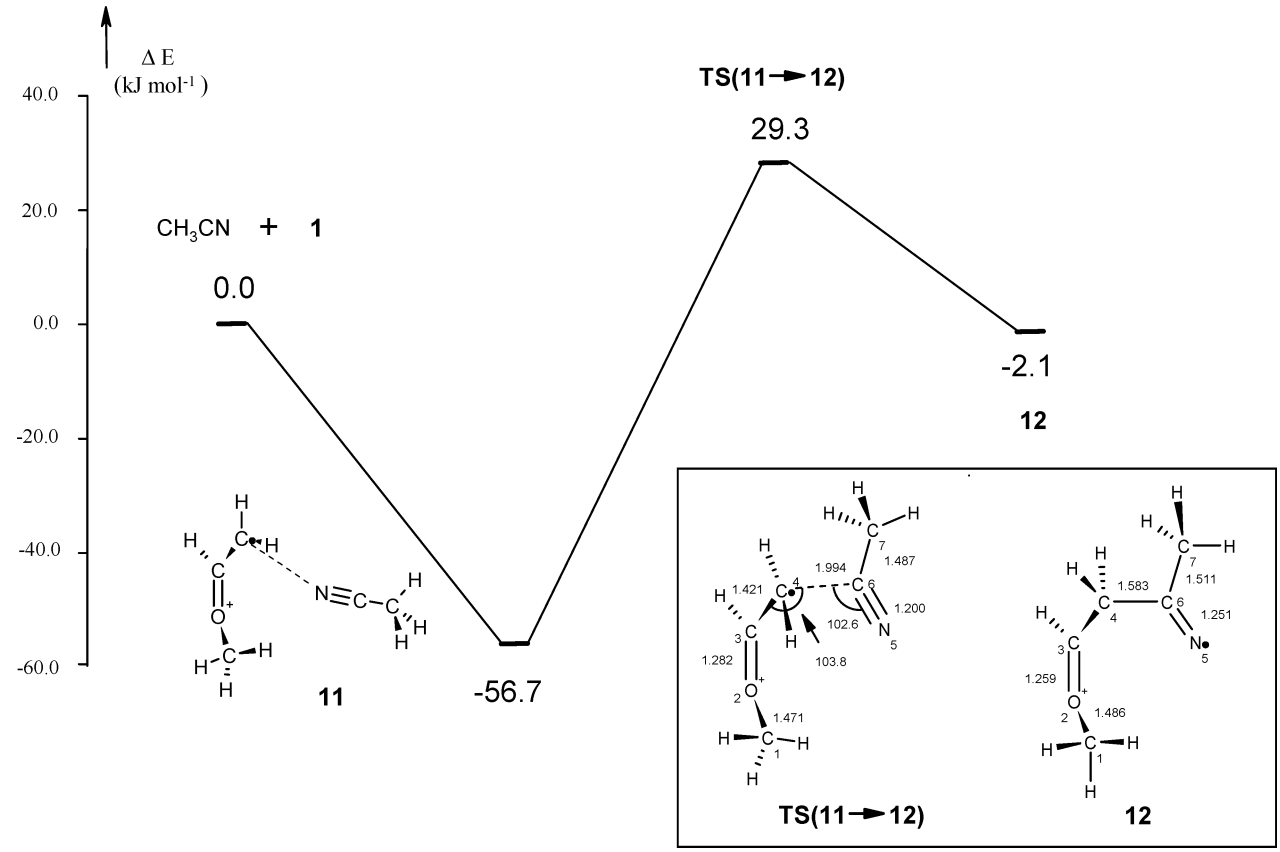


**Figure 4.** G3(MP2) potential energy surface showing the mechanism for reaction 3, $CH_3OCHCH_2^{+\bullet}$ (**1**) + $CH_3CN$ → $CH_3O^+CHCH_2CN^{\bullet}CH_3$ (**12**).

This explains why no ion **1** is produced by simply mixing the *m*/*z* 58 ions fragmented from 1,4-dioxane$^{+\bullet}$ with formaldehyde.

Isomer **1** is often considered to be the radical cation of methyl vinyl ether. However, NBO analysis shows that the $C^3-O^2$ bond (1.287 Å) has considerable double bond character and a significant amount of unpaired spin resides at $C^4$. As a result, the reactions of ion **1** are often initiated by a radical attack at $C^4$.

**3.2. Reaction with Acetonitrile.** The reactions studied in this section are

$$CH_3OCHCH_2^{+\bullet}\ (\mathbf{1}) + CH_3CN \rightarrow CH_3O^+CHCH_2CN^{\bullet}CH_3\ (\mathbf{12}) \quad (3)$$

$$^{\bullet}CH_2CH_2OCH_2^+\ (\mathbf{2}) + CH_3CN \rightarrow {}^{\bullet}CH_2CH_2N^+CCH_3\ (\mathbf{15}) + CH_2O \quad (4)$$

The G3(MP2) profiles of these reactions are displayed in Figures 4 and 5, respectively.

A clue for the existence of a minor isomeric component for the $C_3H_6O^{+\bullet}$ fragment is provided by the result of its reaction with acetonitrile. In the study of Thissen et al., about 5% of the $C_3H_6O^{+\bullet}$ ions remain unreacted in the presence of acetonitrile. The calculated PESs for the respective reactions of **1** and **2** with acetonitrile support the suggestion that the unreacted 5% of $C_3H_6O^{+\bullet}$ ions are the result of the existence of **1**.

*3.2.1. Reaction of **1** and Acetonitrile, Reaction 3.* As can be seen in Figure 4, ion **1** binds with acetonitrile to form a collision complex **11**. The calculated binding energy is 56.7 kJ mol$^{-1}$. However, the amount of energy gained is not sufficient for complex **11** to overcome the barrier for the radical attack on the electrophilic center $C^6$ via **TS(11 → 12)**. The activation energy for such an attack is 86.0 kJ mol$^{-1}$. Though this hypothetical reaction is slightly exothermic, it is kinetically unfavorable. The computational results are in accordance with the observed inertness of ion **1**.

*3.2.2. Reaction of **2** and Acetonitrile, Reaction 4.* Reaction 4 was previously studied by Wittneben et al,[13] but they did not determine which of their two proposed mechanisms is more favorable. In any event, another pathway is suggested in Figure 5, where **2** binds with acetonitrile to form collision complex **13**. This process is exothermic and the binding energy is 71.3 kJ mol$^{-1}$. Upon radical addition via **TS(13 → 14)**, complex **14** is formed. The energy of this TS is 32.5 kJ mol$^{-1}$ below free **2** and acetonitrile. Dissociation of complex **14** yields free formaldehyde and the ionized ethylene transfer product **15**. Unlike ion **2**, the unpaired electron on $C^1$ of **15** has a negligible interaction with $\sigma^*(C^2-N^3)$.

The heat of reaction of this process is −74.6 kJ mol$^{-1}$, which is much more exothermic than reaction 3. These results are in accordance with the observed rapid transfer of ionized ethylene by **2** and the inertness of **1** toward acetonitrile in the experiments conducted by Thissen et al.[17]

**3.3. Reaction with Formaldehyde.** The reactions studied in this section include

$$^{\bullet}CH_2CH_2OCH_2^+\ (\mathbf{2}) + CH_2O \rightarrow C_4H_7O_2^+\ (\mathbf{18a}) + H\ (\mathbf{18b}) \quad (5)$$

$$^{\bullet}CH_2CH_2OCH_2^+\ (\mathbf{2}) + CD_2O \rightarrow {}^{\bullet}CH_2CH_2OCD_2^+\ (\mathbf{2'}) + CH_2O \quad (6)$$

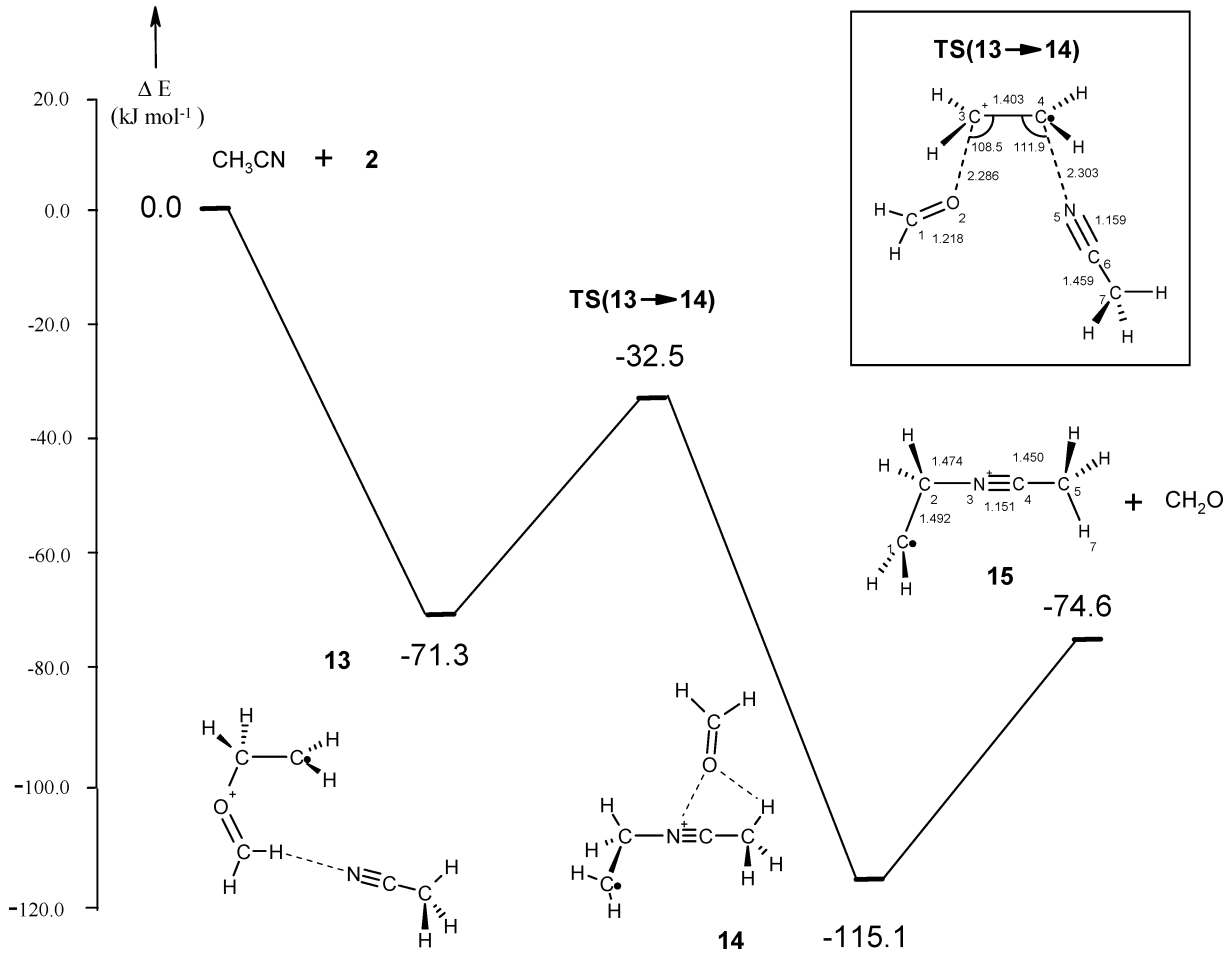


**Figure 5.** G3(MP2) potential energy surface showing the mechanism for reaction 4, $^{\bullet}CH_2CH_2OCH_2^+$ (**2**) + $CH_3CN \rightarrow {}^{\bullet}CH_2CH_2N^+CCH_3$ (**15**) + $CH_2O$.

The G3(MP2) profiles of these reactions are shown in Figures 6 and 7, respectively.

The observed results of the reaction between the $C_3H_6O^{+\bullet}$ ions and formaldehyde also suggest the presence of a minor isomeric component for the *m*/*z* 58 fragments.[17] Now we have established the pathways to explain some of the experimental results.

The reaction of ion **2** with formaldehyde has also been studied by Mourgues et al.[32] experimentally. In the study of Thissen et al.,[17] results similar to those of Mourgues et al.[32] were obtained, except that they found about 10% of the $C_3H_6O^{+\bullet}$ ions remained unreacted. According to the study of Mourgues et al.,[32] ion **2** reacts with formaldehyde through two different pathways. One involves cyclization yielding 1,3-dioxane$^{+\bullet}$, followed by hydrogen radical loss (reaction 5). Another is described as an exchange of the $OCH_2$ portion of the parent ion by an incoming formaldehyde molecule (reaction 6).

*3.3.1. Addition−Cyclization Reaction of **2** with Formaldehyde, Reaction 5.* This process is observed to be the slower of reactions 5 and 6. However, according to the G3(MP2) profile shown in Figure 6, there is no exceedingly high barrier for reaction 5. The reaction starts with the addition of formaldehyde at the cationic carbon in **6b** and proceeds via **TS(6b → 16a)** to form adduct **16a**. The energy cost is so low that **TS(6b → 16a)** is only 4.9 kJ mol$^{-1}$ above complex **6b**. The exceptionally long $C^1-O^5$ (1.822 Å) bond in **16a** is the result of the interaction between the lone pair electrons on $O^2$ and the $\sigma^*(C^1-O^5)$, as revealed by NBO analysis. Such orbital interaction tends to weaken the $C^1-O^5$ bond. By $C^3-O^2$ bond rotation, adduct **16a** can transform into conformer **16b** via **TS(16a → 16b)**, which also involves a low energy barrier. The final cyclization step proceeds via **TS(16b → 17)**, which is 66.0 kJ mol$^{-1}$ below free **2** and formaldehyde.

The formation of 1,3-dioxane$^{+\bullet}$ (**17**) is very exothermic. Nevertheless, subsequent hydrogen radical loss via **TS(17 → 18)** produces an even more stable product pair of **18a** and **18b**. The overall heat of reaction is −124.5 kJ mol$^{-1}$.

*3.3.2. Formaldehyde Exchange Reaction of **2**, Reaction 6.* Intuitively, it is difficult to see why reaction 6 is faster than reaction 5, as the former inevitably involves heterolytic bond cleavage. Hence, it is worth investigating the pathway of reaction 6 theoretically.

For the ionized ethylene transfer to formaldehyde by isomer **2**, our calculations, as summarized in Figure 7, show that it can proceed via intermediate **7**, which has two equivalent partial C−O bonds. The dissociation of the original C−O bond completes the exchange process.

Alternatively, the formaldehyde exchange can also proceed via a TS. This pathway involves the formation of IMC **6a**, which is more stable than the reactants by 63.2 kJ mol$^{-1}$. Afterward, IMC **6a** undergoes formaldehyde exchange via **TS(6a → 6a)**. This process requires an activation energy of 49.3 kJ mol$^{-1}$. Therefore, one would not expect this to be a fast reaction.

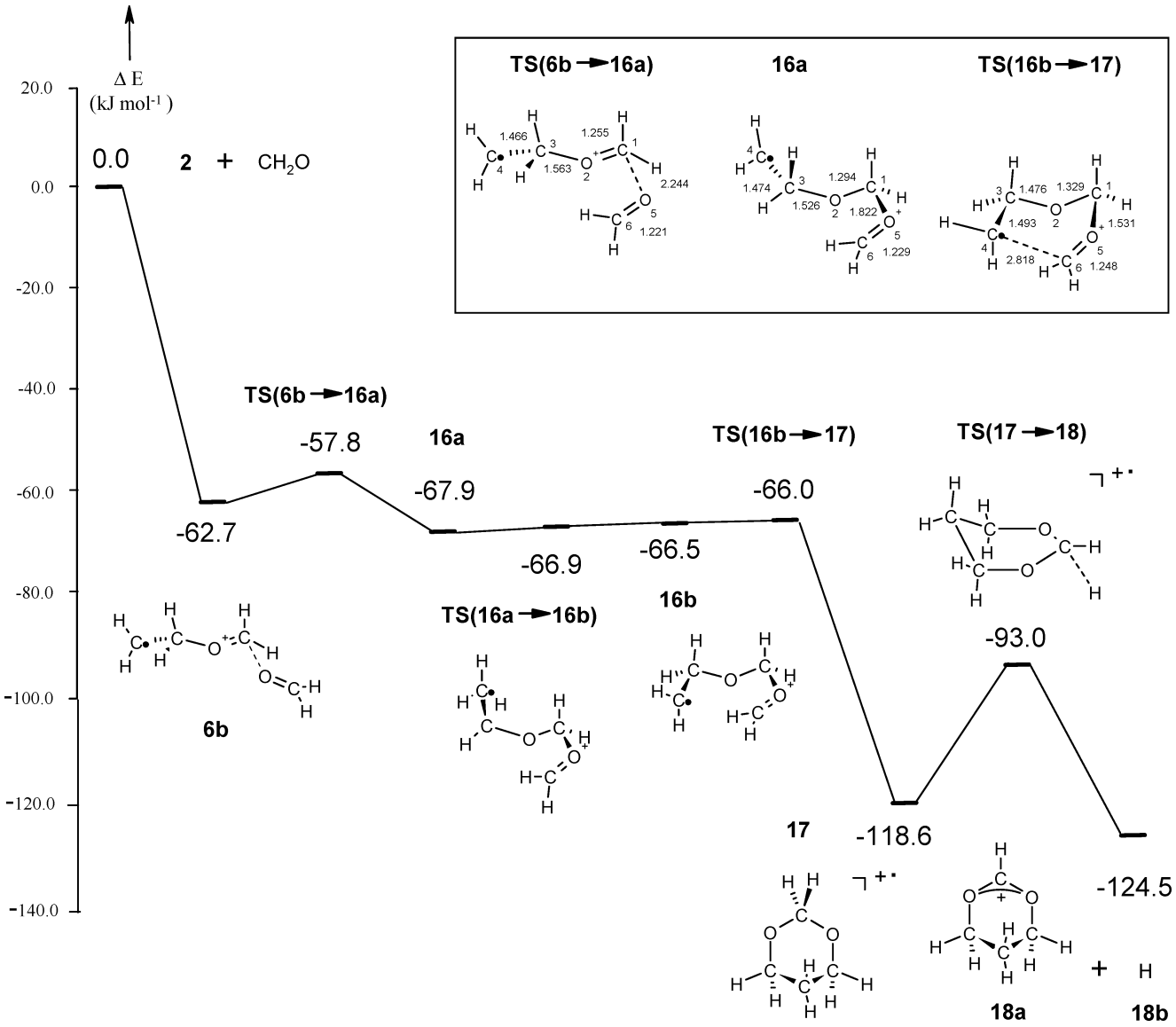


**Figure 6.** G3(MP2) potential energy surface showing the mechanism for reaction 5, $^{\bullet}CH_2CH_2OCH_2^+$ (**2**) + $CH_2O \rightarrow C_4H_7O_2^+$ (**18a**) + H.

However, if we allow an extra formaldehyde molecule to bind with complexes **6a** or **6b**, a larger IMC, **19**, which has a stabilization energy comparable to that of **6a**, is formed. In this IMC, there is bonding interaction between $C^3$ and $O^2$, but none between $C^3$ and $O^7$. Migration of formaldehyde via **TS(19 → 19)** changes the interaction within the complex, resulting in bonding between $C^3$ and $O^7$ but none between $C^3$ and $O^2$. This process involves a very small activation energy of 2.7 kJ $mol^{-1}$. Unfortunately, the pressure in the ICR cell was apparently not high enough to facilitate the trimolecular collision to produce IMC **19**.

None of the three possible pathways for reaction 6 discussed above would unambiguously lead to a faster rate than reaction 5, even though multiple pathways for this reaction may result in a rapid observed rate.

In passing, it is noted that we also calculated the G3(MP2) energy of the hypothetical adduct formed by **1** and formaldehyde. It is 38.0 kJ $mol^{-1}$ above the reactants and 88.3 kJ $mol^{-1}$ above IMC **9**. In view of the instability of this adduct, any reaction between **1** and formaldehyde inevitably involves a high energy barrier and hence is not observed.

**3.4. Reactions with Ethylene.** The reactions studied in this section are

$$CH_3OCHCH_2^{+\bullet}\ (\mathbf{1}) + CD_2CD_2 \rightarrow CH_3OCHCD_2^{+\bullet}\ (\mathbf{1'}) + CH_2CD_2 \quad (7)$$

$$^{\bullet}CH_2CH_2OCH_2^{+}\ (\mathbf{2}) + CD_2CD_2 \rightarrow C_4H_4D_4^{+\bullet}\ (\mathbf{23'}) + CH_2O \quad (8)$$

The G3(MP2) profiles of these reactions are shown in Figures 8 and 9, respectively.

The experimental results of the reactions between $C_3H_6O^{+\bullet}$ fragment ions with ethylene provide very convincing evidence for the existence of isomer **1** as a minor component of the *m*/*z* 58 fragments. The reaction of the $C_3H_6O^{+\bullet}$ fragment ions with deuterated ethylene produces *m*/*z* 60 fragments. More importantly, Thissen et al.[17] successfully differentiated two peaks at *m*/*z* 60.09 and 60.05 at high resolution. The former peak, which is the major one (93 ± 1%), corresponds to the $C_4H_4D_4^{+\bullet}$ ions, while the latter, which is the minor component (7 ± 1%), corresponds to the $C_3H_4D_2O^{+\bullet}$ ions.

*3.4.1. Reaction of **1** and Ethylene, Reaction 7.* The presence of $C_3H_4D_2O^{+\bullet}$ ions as one of the products for this reaction strongly suggests the existence of isomer **1**, which is known to react with deuterated ethylene via a cycloaddition−

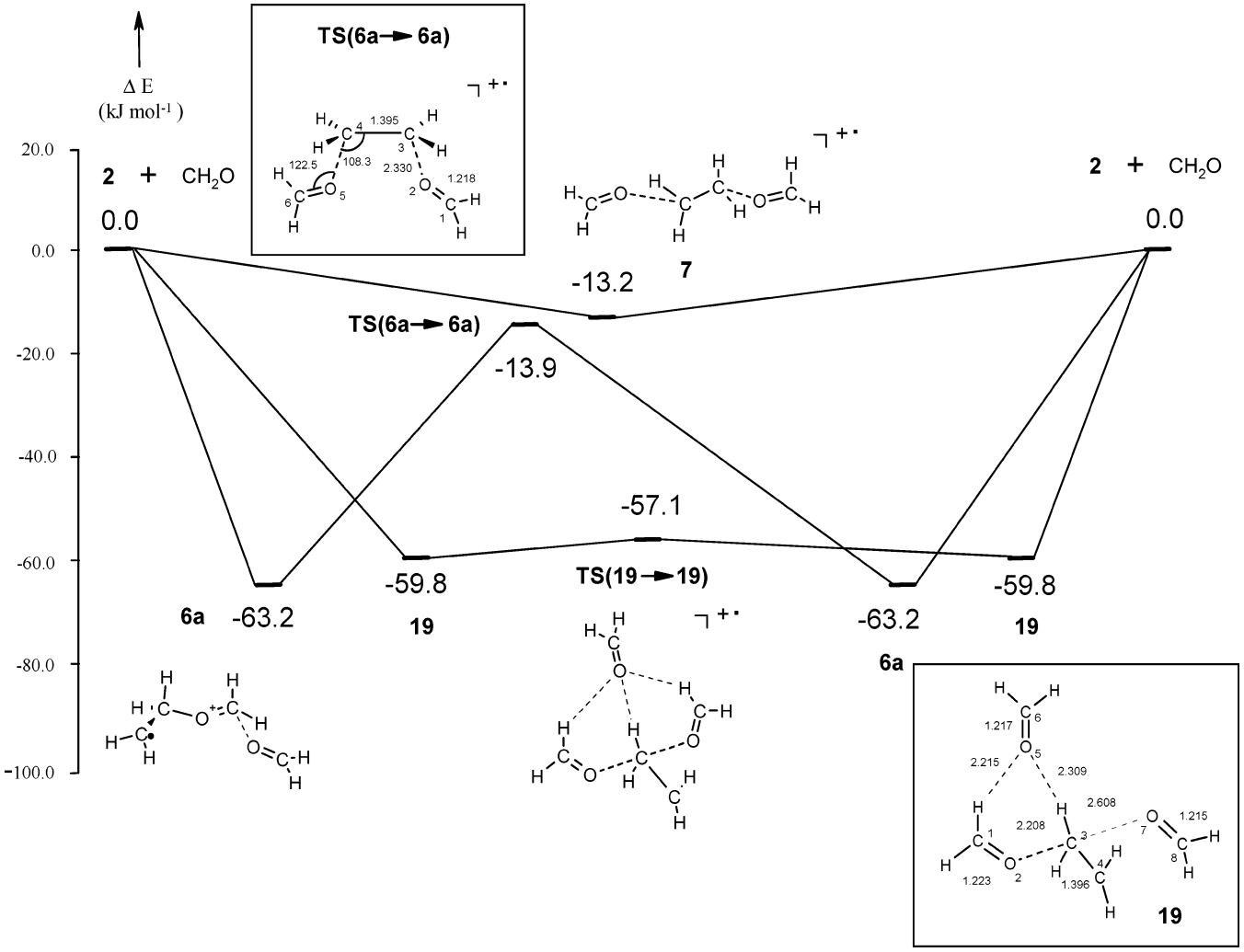


**Figure 7.** G3(MP2) potential energy surface showing the mechanisms for reaction 6, $^{\bullet}CH_2CH_2OCH_2^+$ (**2**) + $CD_2O$ → $^{\bullet}CH_2CH_2OCD_2^+$ (**2′**) + $CH_2O$. Note that the pathway involving **TS(19 → 19)** refers to the reaction $^{\bullet}CH_2CH_2OCH_2^+$ (**2**) + $2CD_2O$ → $^{\bullet}CH_2CH_2OCD_2^+$ (**2′**) + $CH_2O$ + $CD_2O$.

cycloreversion process to yield $CH_3OCHCD_2^{+\bullet}$ (**1′**).[33] Figure 8 illustrates how such an exchange proceeds. To start, **1** combines with ethylene to form IMC **20**. Radical attack on the $\pi$ bond of ethylene at $C^5$ by $C^4$ via **TS(20 → 21)** results in a new C−C bond, yielding intermediate **21**. The G3(MP2) energy of **TS(20 → 21)** is lower than IMC **20** by 2.3 kJ $mol^{-1}$, thus the energy barrier involved is likely to be very small, within the error bar of the G3(MP2) method. Then, ion **21** undergoes a rearrangement via the symmetric **TS(21 → 21)**. The simultaneous formation of the $C^3-C^6$ bond and breaking of the $C^3-C^4$ bond in **TS(21 → 21)** leads to the migration of side chain $C^1-O^2-C^3$ from $C^4$ to $C^6$. The activation energy required is not very high, 33.3 kJ $mol^{-1}$. The subsequent process is simply the reverse of previous steps and the adduct eventually dissociates into deuterated products **1′** and $CH_2CD_2$. It is worth noting that there is no cyclic intermediate involved in these calculations. The G3(MP2) energy profile not only explains the feasibility of reaction 7 but also provides a clear picture for the reaction mechanism.

*3.4.2. Reaction of **2** and Ethylene, Reaction 8.* The major product $C_4H_4D_4^{+\bullet}$ ion is simply the product of ionized ethylene transfer by **2**. As shown in Figure 9, this transfer can proceed in a facile manner similar to that of reaction 6 via intermediate **22**, involving no TS. This intermediate, 16.1 kJ $mol^{-1}$ below the reactants, may be described as a complex formed by formaldehyde, ethylene, and ionized ethylene, with insignificant net bonding among the three units. With formaldehyde dissociated away, the ionized ethylene transfer is complete, yielding $CH_2CH_2CD_2CD_2^{+\bullet}$ (**23′**) as a product.

**3.5. Reaction with propene.** The reactions studied in this section include

$$CH_3OCHCH_2^{+\bullet}\ (\mathbf{1}) + CH_3CHCH_2 \rightarrow CH_3OCHCHCH_3^{+\bullet}\ (\mathbf{27a}) + CH_2CH_2 \quad (9)$$

$$^{\bullet}CH_2CH_2OCH_2^{+}\ (\mathbf{2}) + CH_3CHCH_2 \rightarrow C_5H_{10}^{+\bullet}\ (\mathbf{30}) + CH_2O \quad (10)$$

$$^{\bullet}CH_2CH_2OCH_2^{+}\ (\mathbf{2}) + CH_3CHCH_2 \rightarrow CH_3CH^{\bullet}CH_2OCH_2^{+}\ (\mathbf{35}) + CH_2CH_2 \quad (11)$$

The G3(MP2) profiles of these reactions are displayed in Figures 10, 11, and 12, respectively.

The experimental results of the reactions between the $C_3H_6O^{+\bullet}$ fragment ions and propene are similar to those between the $C_3H_6O^{+\bullet}$ fragment ions and ethylene, but there are some significant differences. In the work of Thissen et al.,[17] two products are formed by reacting the $C_3H_6O^{+\bullet}$ fragments with propene. The major product is the *m/z* 70 fragment $C_5H_{10}^{+\bullet}$ (80%), while the minor one is the *m/z* 72 fragment $C_4H_8O^{+\bullet}$

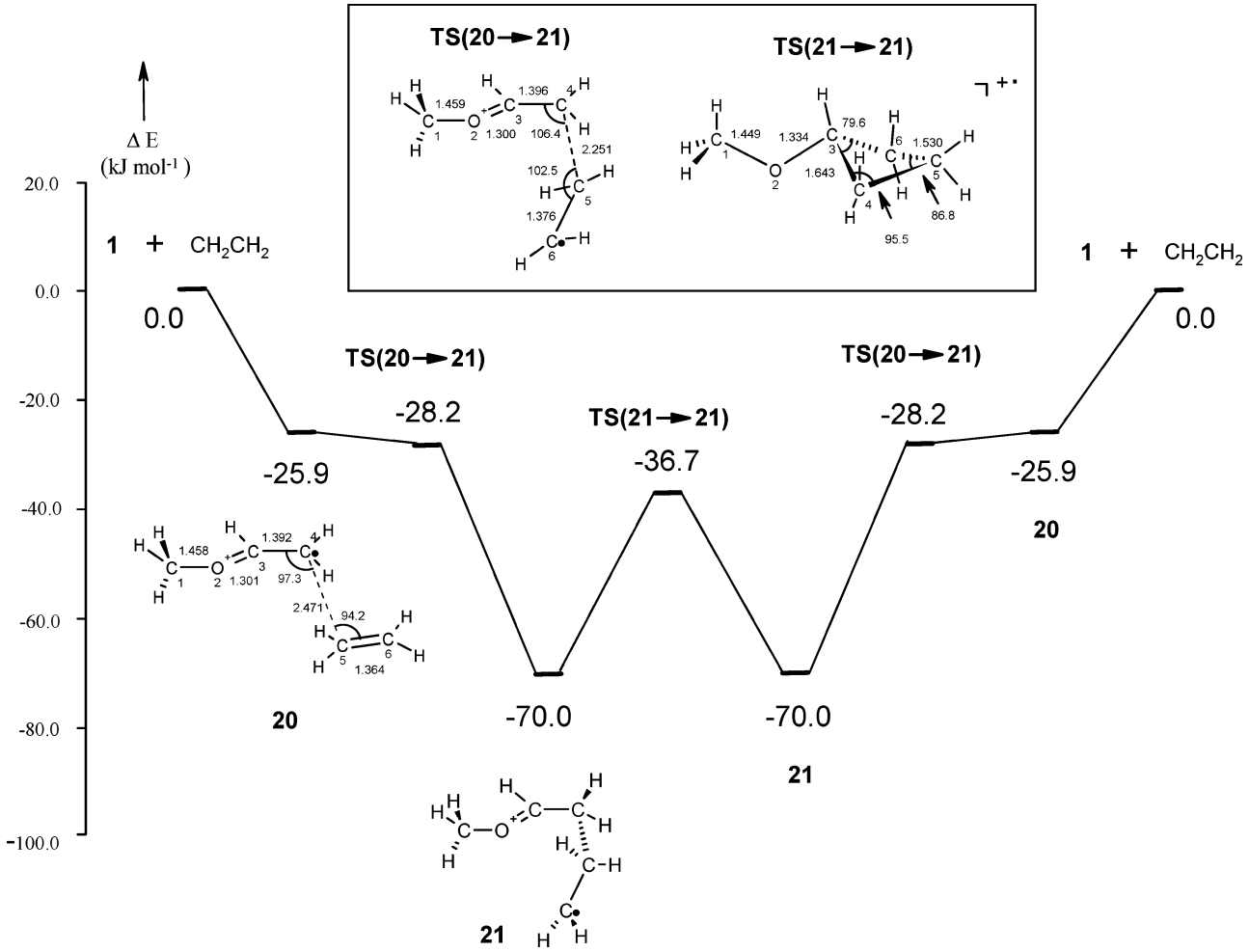


**Figure 8.** G3(MP2) potential energy surface showing the mechanism for reaction 7, $CH_3OCHCH_2^{+\bullet}$ (**1**) + $CD_2CD_2$ → $CH_3OCHCD_2^{+\bullet}$ (**1′**) + $CH_2CD_2$.

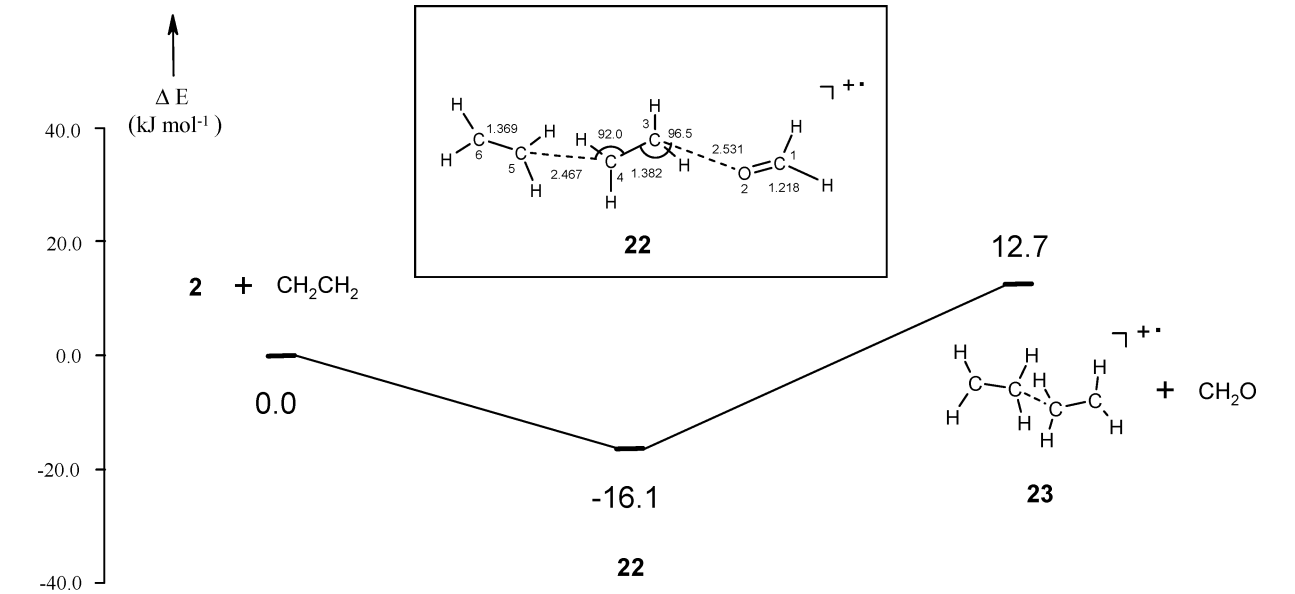


**Figure 9.** G3(MP2) potential energy surface showing the mechanism for reaction 8, $^{\bullet}CH_2CH_2OCH_2^+$ (**2**) + $CD_2CD_2$ → $C_4H_4D_4^{+\bullet}$ (**23′**) + $CH_2O$.

(20%). The former is the expected product of ionized ethylene transfer by **2** (analogous to reaction 8). On the other hand, the *m*/*z* 72 fragment *apparently* is produced by the reaction between **1** and propene via a cycloaddition−cycloreversion process. However, these results, suggesting the presence of 20% of **1**, are inconsistent with those of the other reactions described above. Upon performing a labeling experiment, Thissen et al.[17] discovered that part of the $C_4H_8O^{+\bullet}$ ions are produced by a minor reaction of **2**. However, they were not certain about the reaction mechanism as well as the structure of the product ions.

*3.5.1. Reaction of **1** and Propene, Reaction 9.* The formation of $C_4H_8O^{+\bullet}$ ions as one of the products is in accordance with

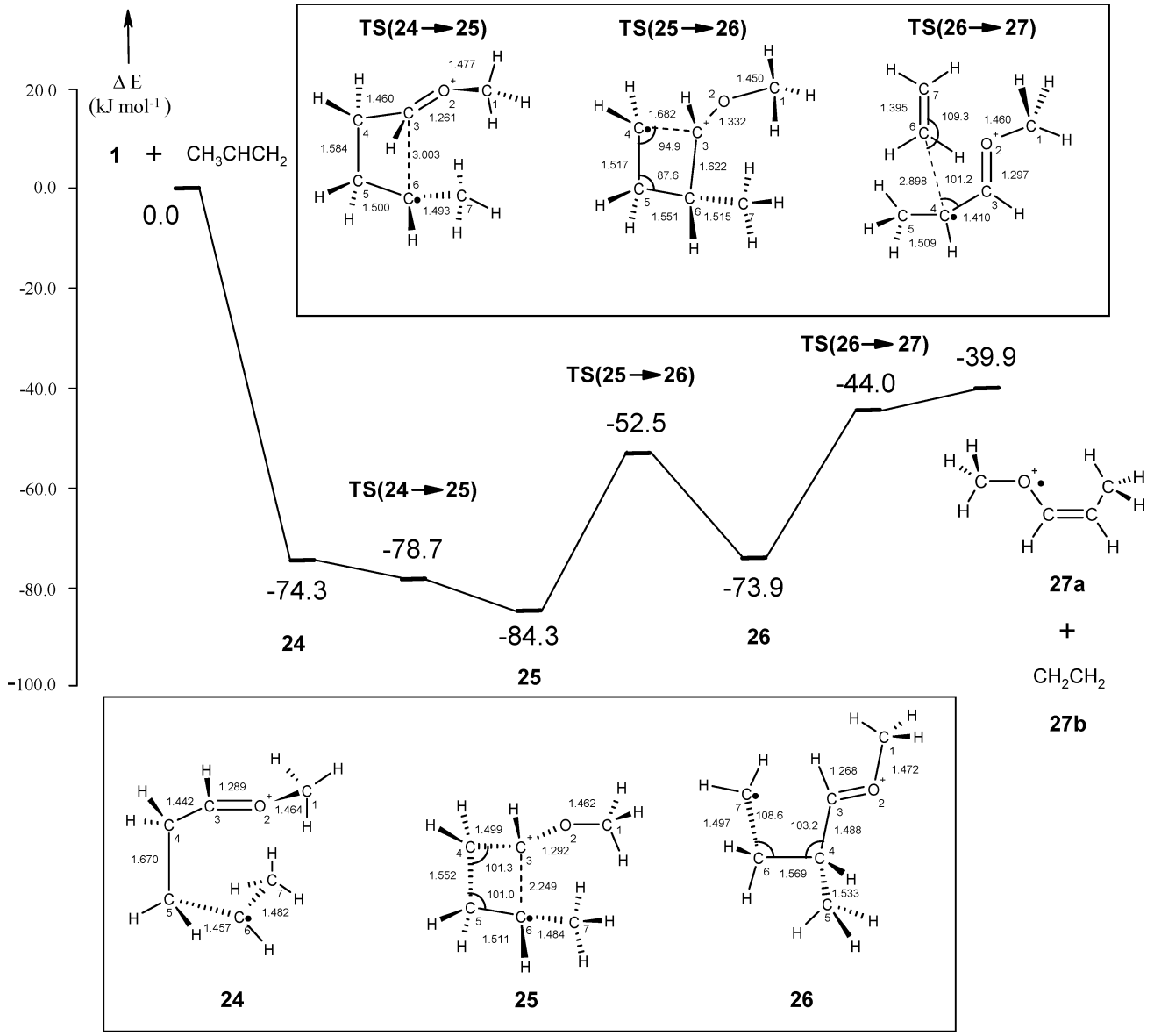


**Figure 10.** G3(MP2) potential energy surface showing the mechanism for reaction 9, $CH_3OCHCH_2^{+\bullet}$ (**1**) + $CH_3CHCH_2$ → $CH_3OCHCHCH_3^{+\bullet}$ (**27a**) + $CH_2CH_2$.

the presence of isomer **1** as a minor component of the *m*/*z* 58 fragments because **1** is known to react with propene to yield $CH_3OCHCHCH_3^{+\bullet}$ (**27a**).[33] This reaction seems to be analogous to reaction 7. However, the G3(MP2) energy profile shown in Figure 10 reveals some key differences between the mechanisms of the two reactions. Unlike reaction 7, ion **1** binds directly with propene to form adduct **24**, which is −74.3 kJ mol$^{-1}$ below the reactants, involving no IMC nor TS. Then **24** cyclizes to form intermediate **25** via **TS(24 → 25)**. The energy barrier involved is again probably so small that it is within the error bar of the G3(MP2) method. The cyclization product, **25**, is 10 kJ mol$^{-1}$ more stable than **24**. In cyclic species **25**, the $C^3-C^6$ bond length is as long as 2.249 Å because it is a one-electron bond, according to NBO analysis. As previously described, no similar intermediate, with a cyclobutane-like framework, exists in the pathway of reaction 7. Subsequently, ion **25** undergoes ring-opening via **TS(25 → 26)** to yield ion **26**, which is almost as stable as **24**. This process requires an activation energy of 31.8 kJ mol$^{-1}$. By the dissociation of the $C^4-C^6$ bond in **26**, ion **27a** and ethylene (**27b**) are produced. The overall exothermicity of this reaction is 39.9 kJ mol$^{-1}$. In view of this exothermicity and the lack of a substantial barrier, reaction 9 is expected to be observed experimentally.

*3.5.2. Reaction of **2** and Propene, Reactions 10 and 11.* The major product, the $C_5H_{10}^{+\bullet}$ ion, produced when **2** reacts with propene, is similar to the $C_4H_4D_4^{+\bullet}$ ion formed in reaction 8; both are products of ionized ethylene transfer by **2**. According to the G3(MP2) energy profile for reaction 10 displayed in Figure 11, the ionized ethylene transfer to propene by ion **2** proceeds in a manner that is slightly different from the pathway shown in Figure 9. Now ion **2** binds directly with propene involving no TS to yield adduct **28**, in which the formation of the new C−C bond does not weaken the C−O bond. Adduct **28** is so stable that it is 98.1 kJ mol$^{-1}$ below the reactants. Afterward, species **28** undergoes C−O bond cleavage via **TS(28 → 29)** to yield IMC **29**, involving an energy barrier of 41.9 kJ mol$^{-1}$. Finally IMC **29** dissociates into $CH_3CHCH_2CH_2CH_2^{+\bullet}$ (**30**) and formaldehyde. The overall exothermicity of this reaction is 27.2 kJ mol$^{-1}$.

An alternative pathway for this reaction is also shown in Figure 11. In this mechanism, **2** and propene first form adduct **31** which is a conformer of **28** and has a very similar stability.

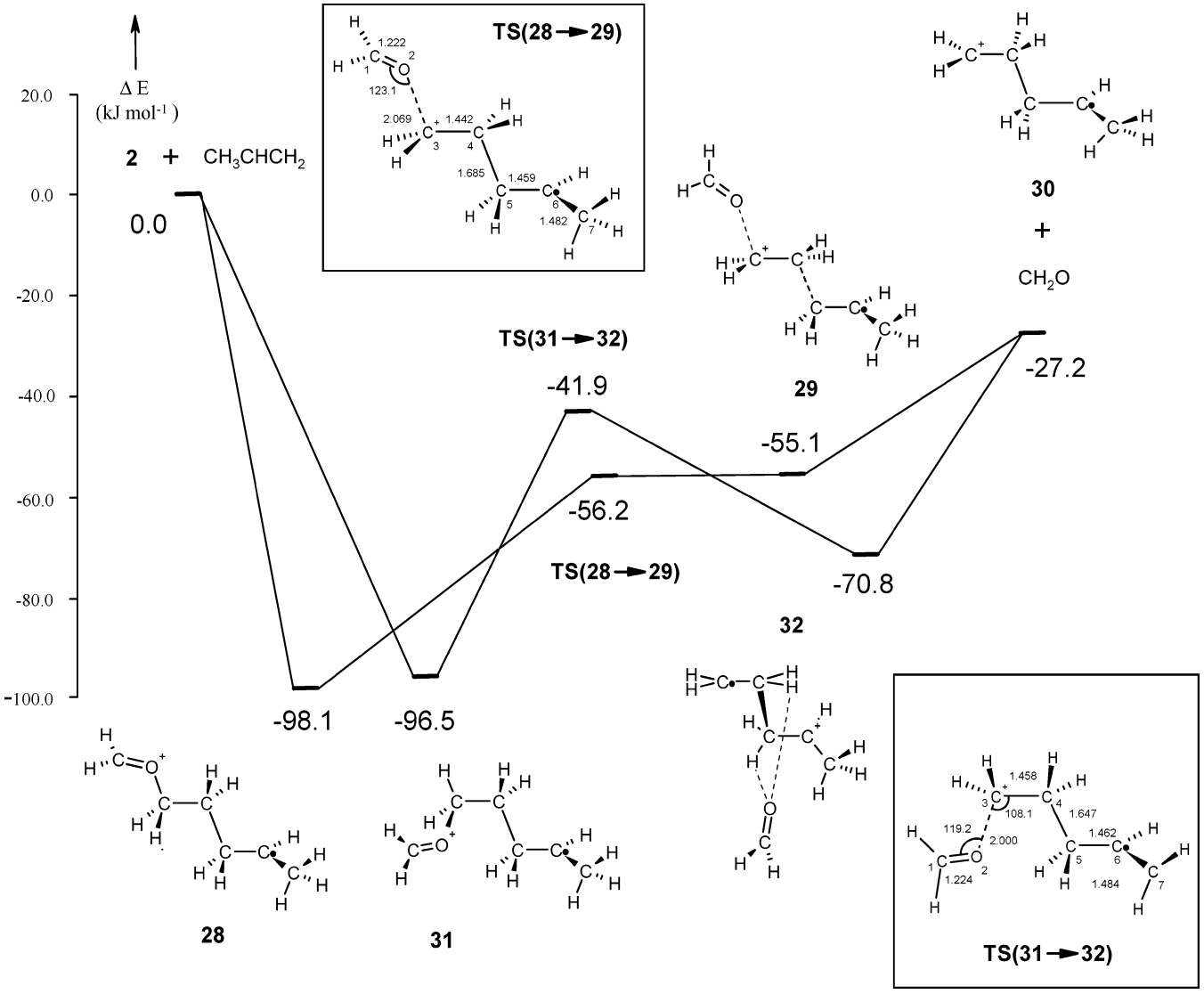


**Figure 11.** G3(MP2) potential energy surface showing the mechanisms for reaction 10, $^{\bullet}CH_2CH_2OCH_2^+$ (**2**) + $CH_3CHCH_2$ → $C_5H_{10}^{+\bullet}$ (**30**) + $CH_2O$.

Subsequently, the C−O bond in **31** cleaves via **TS(31 → 32)** to yield IMC **32**; the barrier of this process is 54.6 kJ mol$^{-1}$. Finally IMC **32** dissociates into $CH_3CHCH_2CH_2CH_2^{+\bullet}$ (**30**) and formaldehyde. As can been seen in Figure 11, the pathways producing the same products are quite similar.

In the labeling experiment conducted by Thissen et al.,[17] the $C_3D_6O^{+\bullet}$ ions fragmented from ionized 1,4-dioxane-$d_8$ reacting with propene does not yield $C_4H_4D_4O^{+\bullet}$ (*m*/*z* 76), which is the expected product from reaction 9. Instead, $C_4H_6D_2O^{+\bullet}$ (*m*/*z* 74) is formed. This result not only suggests that the absence of deuterated isomer **1** in the $C_3D_6O^{+\bullet}$ fragments but also a minor reaction yielding $C_4H_6D_2O^{+\bullet}$ by deuterated **2**. This minor process contributes the extra amount of $C_4H_8O^{+\bullet}$ ions produced, resulting in an apparent inconsistency in the relative composition of isomer **1** in the $C_3H_6O^{+\bullet}$ ions fragmented from ionized 1,4-dioxane. Our calculations suggest a plausible mechanism for this minor reaction.

This reaction, called reaction 11, has the G3(MP2) energy profile shown in Figure 12. Note that this pathway starts with the reactant **30** and formaldehyde (i.e., the products of reaction 10). In this mechanism, formaldehyde and **30** recombine to form IMC **33**, which is −67.5 kJ mol$^{-1}$ below the energy total of **2** and propene. Afterward, IMC **33** undergoes $C^5-C^6$ bond breaking via **TS(33 → 34)**, yielding IMC **34**. The activation energy required is 7.6 kJ mol$^{-1}$. IMC **34**, which is −55.4 kJ mol$^{-1}$ below the energy of **2** and propene, is essentially formed by ethylene, ionized propene, and formaldehyde. Dissociation of IMC **34** yields $CH_3CH^{\bullet}CH_2OCH_2^+$ (**35**) and ethylene. This final process involves an energy barrier of 49.7 kJ mol$^{-1}$, and this is the largest barrier encountered in this reaction pathway. Though this barrier is comparable to the largest energy barrier involved in reaction 10, reaction 11 is less exothermic than the former. Therefore, reaction 11 is only a minor process for isomer **2**.

## 4. Conclusion

In this work, G3(MP2) calculations were carried out to study the fragmentation reactions of ionized 1,4-dioxane as well as the reactions between various reactants (including acetonitrile, formaldehyde, ethylene, and propene) and the isomers $CH_3OCHCH_2^{+\bullet}$ (**1**) and $^{\bullet}CH_2CH_2OCH_2^+$ (**2**) of the $C_3H_6O^{+\bullet}$ ions fragmented from ionized 1,4-dioxane. The calculated results clearly show the following.

(1) In the fragmentation reaction of ionized 1,4-dioxane, both **1** and **2** are formed. In addition, the formation of **1** involves a large energy barrier. Hence **2** appears as a major component (90−95%) and **1** as a minor component (5−10%) of the

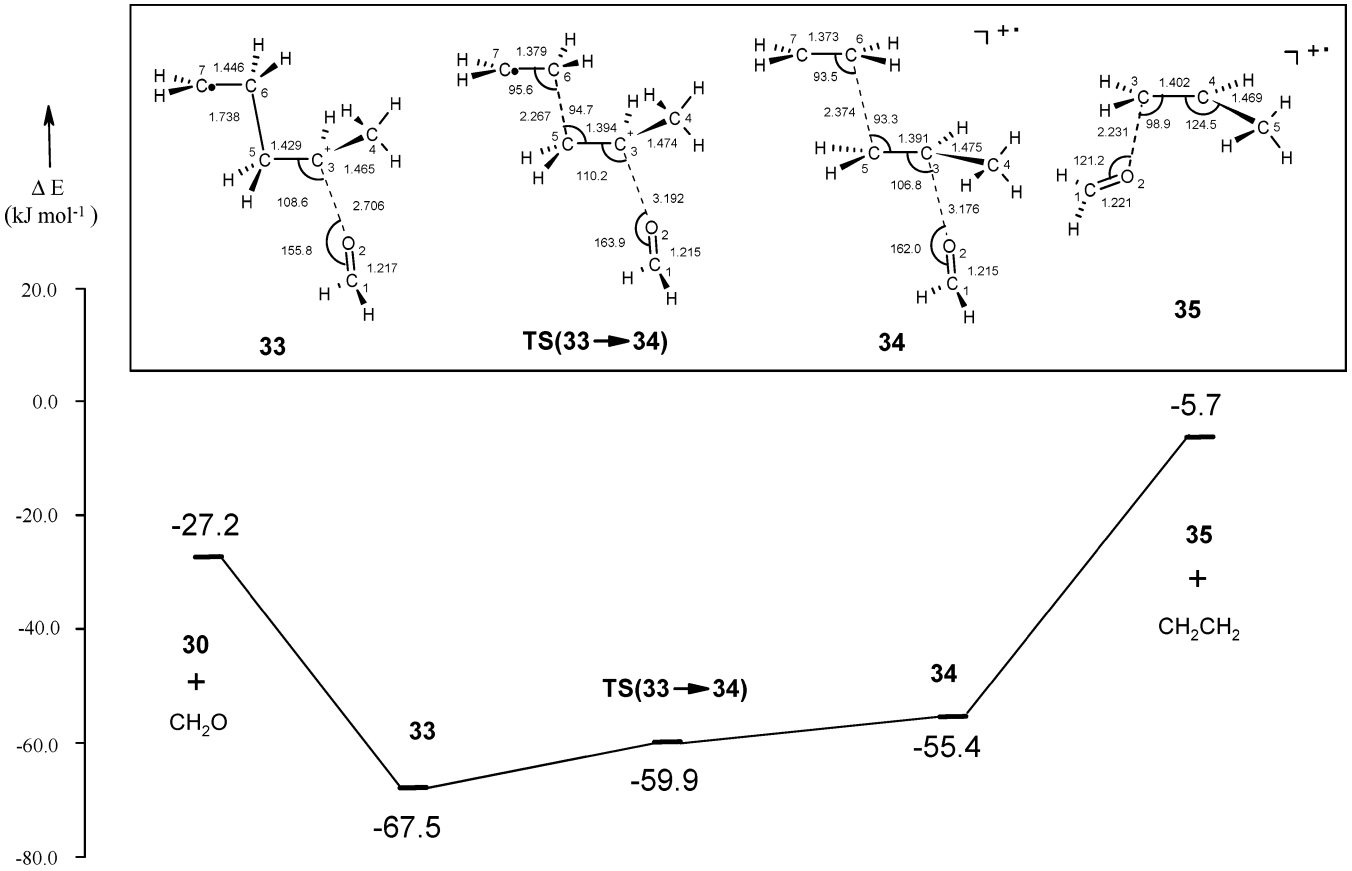


**Figure 12.** G3(MP2) potential energy surface showing the mechanism for reaction 11, $^{\bullet}CH_2CH_2OCH_2^+$ (**2**) + $CH_3CHCH_2 \rightarrow CH_3CH^{\bullet}CH_2OCH_2^+$ (**35**) + $CH_2CH_2$.

$C_3H_6O^{+\bullet}$ ions. In addition, our calculations do not support the formaldehyde-catalyzed pathway for producing **1** suggested by Thissen et al.[17] Instead, we identified an alternative pathway which features a hydrogen-shift TS [**TS(4a → 10)**] prior to the formation of IMC **6a**.

(2) When isomer **2** reacts with the four aforementioned reactants, it readily undergoes ionized ethylene transfer, requiring a small or no energy barrier. Hence the products of these four reactions are observed experimentally.

(3) On the other hand, the reactions between isomer **1** and acetonitrile or formaldehyde involve much higher energy barriers. Hence these reactions are not detected experimentally. Meanwhile, the reactions between **1** and ethylene or propene proceed along the cycloaddition−cycloreversion mechanism involving no overall energy barriers. Hence the expected products are also observed experimentally.

Our calculations show that there is an additional but minor reaction between isomer **2** and propene. This reaction produces $CH_3CH^{\bullet}CH_2OCH_2^+$ (**35**), an isomer of the product $CH_3OCHCHCH_3^{+\bullet}$ (**27a**), formed when **1** reacts with propene. The presence of this minor reaction between **2** and propene explains why there is a 20% $C_4H_8O^{+\bullet}$ minor product, instead of the expected 5−10%, formed in the reaction between the $C_3H_6O^{+\bullet}$ ions and propene.

**Acknowledgment.** This work was supported by a grant from the Research Grants Council of the Hong Kong Special Administrative Region (Project No. CUHK4275/00P). The authors are grateful to an anonymous donor who made a donation to the Department of Chemistry at the Chinese University of Hong Kong. The generous allocation of computer time on the IBM RS/6000 SP High Performance Computer Cluster in the Computer Service Center at the Chinese University of Hong Kong is much appreciated.

**Supporting Information Available:** Optimized structures of all species involved in the reactions studied as well as the G3(MP2) energetic data ($E_0$ and $H_{298}$) of the species. This material is available free of charge via the Internet at http://pubs.acs.org.

## References and Notes

(1) Luippold, D. A.; Beauchamp, J. L. *J. Phys. Chem.* **1976**, *80*, 795.
(2) Allinger, N. L.; Hickey, M. J. *THEOCHEM* **1973**, *17*, 233.
(3) Allinger, N. L.; Hickey, M. J. *Tetrahedron* **1972**, *28*, 2157.
(4) Bouma, W. J.; MacLeod, J. K.; Radom, L. *J. Am. Chem. Soc.* **1980**, *102*, 2246.
(5) Fausto, R.; Teixeira-Dias, J. J. C.; Carey, P. R. *THEOCHEM* **1988**, *168*, 179.
(6) Kroto, H. W.; Landsberg, B. M.; Suffolk, R. J.; Vodden, A. *Chem. Phys. Lett.* **1974**, *29*, 265.
(7) Bouchoux, G.; Luna, A.; Tortajada, J. *Int. J. Mass Spectrom. Ion Processes* **1997**, *167/168*, 353.
(8) Polce, M. J.; Wesdemiotis, C. *J. Am. Soc. Mass Spectrom.* **1996**, *7*, 573.
(9) Fraser-Monteiro, M. L.; Fraser-Monteiro, L.; Butler, J. J.; Baer, T.; Haas, J. R. *J. Phys. Chem.* **1982**, *86*, 739.
(10) Dannacher, J.; Stadelmann, J.-P. *Int. J. Mass Spectrom.* **2001**, *208*, 147.
(11) Polce, M. J.; Wesdemiotis, C. *J. Am. Soc. Mass Spectrom.* **1995**, *6*, 1030.
(12) Bouchoux, G.; Tortajada, J. *Rapid Commun. Mass Spectrom.* **1987**, *1*, 86.
(13) Wittneben, D.; Grützmacher, H.-F. *Int. J. Mass Spectrom. Ion Processes* **1990**, *100*, 545.
(14) Kiminkinen, L. K. M.; Stirk, K. G.; Kenttämaa, H. I. *J. Am. Chem. Soc.* **1992**, *114*, 2027.
(15) Polce, M. J.; Wesdemiotis, C. *J. Am. Chem. Soc.* **1993**, *115*, 10849.

(16) Smith, R. L.; Chou, P. K.; Kenttämaa, H. I. In *The Structure, Energetics and Dynamics of Organic Ions*; Baer, T., Ng, C.-Y., Powis, I., Eds.; Wiley: Chichester, U.K., 1996; p 197.

(17) Thissen, R.; Audier, H. E.; Chamot-Rooke, J.; Mourgues, P. *Eur. Mass Spectrom.* **1999**, *5*, 147.

(18) Curtiss, L. A.; Redfern, P. C.; Raghavachari, K.; Rassolov, V. R.; Pople, J. A. *J. Chem. Phys.* **1999**, *110*, 4073.

(19) Lau, J. K.-C.; Li, W.-K.; Chiu, S.-W. *J. Phys. Chem. A* **2001**, *105*, 10816.

(20) Cheng, M.-F.; Li, W.-K. *J. Phys. Chem. A* **2003**, *107*, 5492.

(21) Ho, H.-O.; Li, W.-K. *THEOCHEM* **2004**, *712*, 49.

(22) Frisch, M. J.; Trucks, G. W.; Schlegel, H. B.; Scuseria, G. E.; Robb, M. A.; Cheeseman, J. R.; Montgomery, J. A., Jr.; Vreven, T.; Kudin, K. N.; Burant, J. C.; Millam, J. M.; Iyengar, S. S.; Tomasi, J.; Barone, V.; Mennucci, B.; Cossi, M.; Scalmani, G.; Rega, N.; Petersson, G. A.; Nakatsuji, H.; Hada, M.; Ehara, M.; Toyota, K.; Fukuda, R.; Hasegawa, J.; Ishida, M.; Nakajima, T.; Honda, Y.; Kitao, O.; Nakai, H.; Klene, M.; Li, X.; Knox, J. E.; Hratchian, H. P.; Cross, J. B.; Bakken, V.; Adamo, C.; Jaramillo, J.; Gomperts, R.; Stratmann, R. E.; Yazyev, O.; Austin, A. J.; Cammi, R.; Pomelli, C.; Ochterski, J. W.; Ayala, P. Y.; Morokuma, K.; Voth, G. A.; Salvador, P.; Dannenberg, J. J.; Zakrzewski, V. G.; Dapprich, S.; Daniels, A. D.; Strain, M. C.; Farkas, O.; Malick, D. K.; Rabuck, A. D.; Raghavachari, K.; Foresman, J. B.; Ortiz, J. V.; Cui, Q.; Baboul, A. G.; Clifford, S.; Cioslowski, J.; Stefanov, B. B.; Liu, G.; Liashenko, A.; Piskorz, P.; Komaromi, I.; Martin, R. L.; Fox, D. J.; Keith, T.; Al-Laham, M. A.; Peng, C. Y.; Nanayakkara, A.; Challacombe, M.; Gill, P. M. W.; Johnson, B.; Chen, W.; Wong, M. W.; Gonzalez, C.; Pople, J. A. *Gaussian 03*, revision B.05; Gaussian, Inc.: Wallingford, CT, 2004.

(23) Becke, A. D. *J. Chem. Phys.* **1993**, *98*, 5648.

(24) Stephens, P. J.; Devlin, F. J.; Chabalowski, C. F.; Frisch, M. J. *J. Phys. Chem.* **1994**, *98*, 11623.

(25) Bak, K. L.; Devlin, F. J.; Ashvar, C. S.; Taylor, P. R.; Frisch, M. J.; Stephens, P. J. *J. Phys. Chem.* **1995**, *99*, 14918.

(26) Lee, C.; Yang, W.; Parr, R. G. *Phys. Rev. B* **1988**, *37*, 785.

(27) Gonzalez, C.; Schlegel, H. B. *J. Chem. Phys.* **1989**, *90*, 2154.

(28) Gonzalez, C.; Schlegel, H. B. *J. Chem. Phys.* **1990**, *94*, 5523.

(29) Reeds, A. E.; Curtiss, L. A.; Weinhold, F. *Chem. Rev.* **1988**, *88*, 899.

(30) Burrill, A. B.; Johnson, P. M. *Chem. Phys. Lett.* **2001**, *350*, 473.

(31) Carey, F. A.; Sundberg, R. J. *Advanced Organic Chemistry, Part A: Structure and Mechanism*, 4th ed.; Kluwer Academic/Plenum Publishers: New York, 2000, 1996; p 222.

(32) Mourgues, P.; Audier, H. E.; Hammerum, S. *Rapid Commun. Mass Spectrom.* **1994**, *8*, 53.

(33) Dass, C. *Mass Spectrom. Rev.* **1990**, *9*, 1.